Cyclic Triaxial Tests on Deformation Properties of Softrocks

by

J. Koseki [1], H. Indo [2], K. Hayano [3], T. Sato [4] and M. Torimitsu [5]

ABSTRACT

Undrained cyclic triaxial tests were performed on two kinds of sedimentary softrocks (the Kazusa group). Mudstone samples were retrieved from a depth of about 80 m at the Sagamihara experimental site, and silt-sandstone samples were retrieved from a depth of about 60 m below the seabed at an offshore site near the mouth of Tokyo Bay. A saturated cylindrical specimen of 5 cm in diameter and about 12 cm in height was isotropically re-consolidated to the in-situ effective overburden stress. After applying an initial deviator stress under drained condition, undrained cyclic axial loading was performed, which was followed by monotonic axial loading while maintaining the undrained condition. Observed behaviors on the accumulation of residual axial strains during the undrained cyclic loading and on the effects of the cyclic loading history on the maximum deviator stress during the subsequent monotonic loading are compared between the two kinds of samples. An attempt is also made to simulate the residual deformation behavior of the silt-sandstone samples during the cyclic loading.

INTRODUCTION

In Japan, sedimentary softrock deposits have been considered as one of stiff subsoil layers that can support large scaled civil engineering structures and buildings. In fact, one abutment (1A) and another pier (3P) of Akashi Kaikyo Bridge having a central span of 1990 m are supported by a sedimentary softrock deposit of Early Neogene Period (Kobe Group), which survived the 1995 Hyogoken-Nanbu earthquake with exhibiting only a limited amount of residual deformations and displacements (Yamagata et al., 1996).

[1] Junichi Koseki, Associate Professor, Institute of Industrial Science, University of Tokyo

[2] Hiroki Indo, Engineer, Aichi Prefecture (Formerly, Graduate Student, University of Tokyo)

[3] Kimitoshi Hayano, Researcher, Port and Airport Research Institute (Formerly, Research Associate, IIS, Univ. of Tokyo)

[4] Takeshi Sato, Research Associate, IIS, Univ. of Tokyo

[5] Michie Torimitsu, Technical Staff, ditto

In the performance-based designs of the above subsoil-structure systems against large earthquake loads, such as those observed during the 1995 Hyogoken-Nanbu earthquake, their residual deformations after the earthquake need to be properly evaluated. When excessively conservative design procedures are adopted, however, they often yield unrealistically large residual deformations. On the other hand, it was also reported that the residual deformations of subsoils supporting two piers of Akashi Kaikyo Bridge could be simulated to a certain extent by modeling their residual deformation properties based on relevant laboratory test results (Koseki, et al., 2001; Kashima et al., 2000). It is to be noted that the deformation behaviors of softrocks under large earthquake loads are not well understood, since the number of relevant laboratory tests is very limited (Okamura et al., 1999).

In view of the above, in the present study, a series of undrained cyclic triaxial tests was performed on two kinds of sedimentary softrocks in order to investigate into their deformation properties when subjected to large amplitude undrained cyclic loading.

TESTED MATERIALS AND TESTING PROCEDURES

A series of core samples of mudstone were obtained from a layer of Kazusa group by hand-operated direct core sampling using a 5 cm diameter diamond core barrel at a depth of about 80 m inside a deep shaft at the Sagamihara experimental site (Tatsuoka et al., 1997; Nakanishi et al., 1998). The mean diameter was about 0.02 mm after thorough crushing, and the initial water content was around 35 %.

Another series of core samples of silt-sandstone were retrieved from a layer of Kazusa group by rotary core tube drilling at a depth of about 60 m below the seabed at an offshore site near the mouth of Tokyo Bay. The mean diameter was 0.06 to 0.08 mm after thorough crushing, and the initial water content was around 25 %.

A cylindrical specimen of 5 cm in diameter and about 12 cm in height was trimmed and set on a triaxial testing system with a gear-type axial loading device (Hayano et al., 2001). It was fully saturated by vacuuming and back-pressurizing to 294 kPa in a triaxial cell filled with de-aired water (Ampadu and Tatsuoka, 1993). Both ends of the specimen were capped with gypsum on-site in the triaxial cell to ensure a good contact with the stainless platens attached to the speciment cap and pedestal. To facilitate drainage from the specimen during saturation and consolidation processes, a side drain of filter paper was used.

From an initial confining stress of 29.4 kPa, the specimen was isotropically re-consolidated to the in-situ effective overburden stress (785 kPa for the mudstone samples and 589 kPa for the silt-sandstone samples). In order to simulate qualitatively the application of vertical loads due to construction of huge foundations, the effective vertical stress σ_v' was increased under drained condition. Then, undrained cyclic axial loading was performed, and finally the axial load was monotonically increased while maintaining the undrained condition. The initial deviator stress q_0

($=\sigma_{v0}' - \sigma_{h0}'$) before undrained cyclic shearing was set at about 50 to 60 % of the peak deviator stress that was measured by undrained monotonic axial loading tests without cyclic loading conducted under otherwise the same conditions. Refer to Fig. 1 for typical results and definitions of other stress parameters. In order to measure the axial strain accurately, a set of local deformation transducers (LDTs) were employed.

At several states in the course of the isotropic re-consolidation, a set of small amplitude drained axial loading and unloading was conducted to evaluate the quasi-elastic vertical Young's moduli at a strain level of about 0.001%. Similarly, during the process of the drained monotonic loading and the undrained cyclic loading, a set of small amplitude axial unloading and reloading was conducted under drained and undrained conditions, respectively, at several states, for example at state b in Fig. 1.

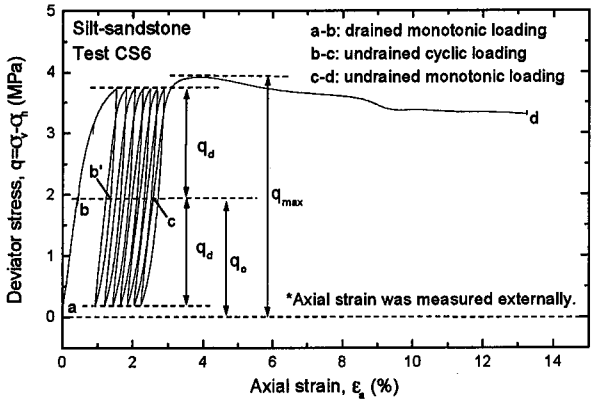

Fig.1. Typical stress-strain relationship and definition of stress parameters (for test CS6 on silt-sandstone sample)

RESULTS AND DISCUSSIONS

Residual axial strains of mudstone samples during undrained cyclic loading

On the mudstone samples, seven undrained cyclic triaxial tests were performed under different stress conditions in terms of the initial deviator stress q_0 and the cyclic deviator stress q_d. Values of residual axial strains ε_r measured at a stress state of $q=q_0$ during each cycle, which include those accumulated during the initial application of q_0 under drained condition, are plotted versus the number of cycles in Fig. 2. It should be noted that the ε_r values are evaluated from the average values of axial strains measured with two LDTs. In general, accumulation of the ε_r values during undrained cyclic loading was to a limited extent, except for the test result of CY3 yielding a sudden large accumulation of ε_r after the number of cycles exceeded about 10 or 15.

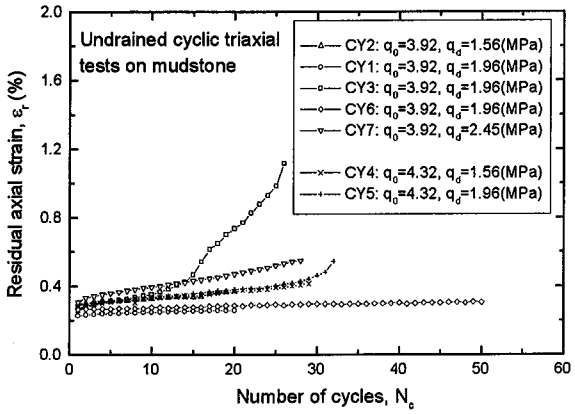

Fig.2. Accumulation of residual axial strains during cyclic loading on mudstone samples

Stress-strain relationships for test CY3 are shown in Fig. 3. The sudden large accumulation of the axial strain was measured only with one LDT (LDT1 in Fig. 3a) set in the region crossing the shear band, which was observed at the time of reassembling the apparatus and the specimen. On the other hand, with the other LDT (LDT2) not crossing the shear band, a much smaller amount of accumulation of the axial strain was measured. These different behaviors suggest that the sudden large accumulation of residual deformation took place mainly within the shear band, which was possibly formed at the same moment as the residual deformation started to accumulate during the undrained cyclic loading, while the other part of the specimen suffered residual deformation to a much lesser extent. Similar behavior was also observed in test CY5 that started to yield a large value of ε_r after the number of cycles exceeded about 30 (Fig. 2). It should be noted, however, that, with visual observation of the side of the specimen covered with membrane, the exact moment when the shear band was formed could not be evaluated.

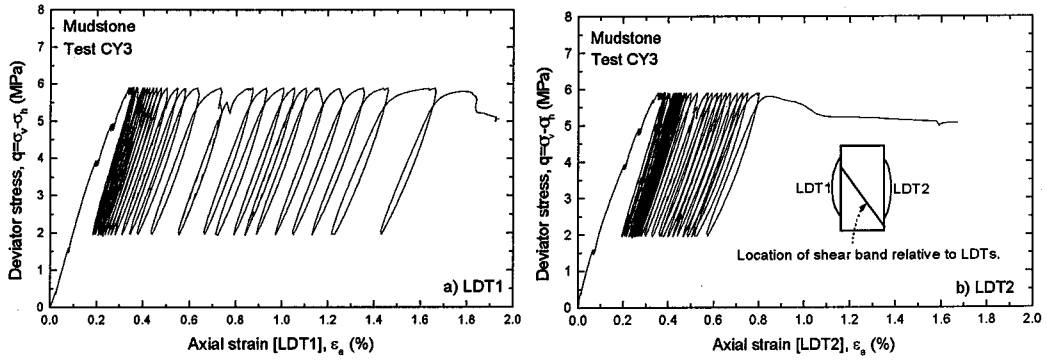

Fig.3. Stress-strain relationships for test CY3 on mudstone sample

Figure 4 shows stress-strain relationships for test CY7 that yielded gradual accumulation of ε_r throughout the undrained cyclic loading with the largest q_d value among all the tests. The axial strain measured with LDT1 that crossed the observed shear band (Fig. 4a) was generally larger than the other, while the difference in these measured values were not significant. This suggests that the specimen suffered residual deformation relatively uniformly, while a limited extent of strain localization may have taken place within a region corresponding to the shear band that was formed in the subsequent monotonic loading stage. Similar behavior was also observed in the other tests, excluding tests CY3 and CY5 as mentioned above.

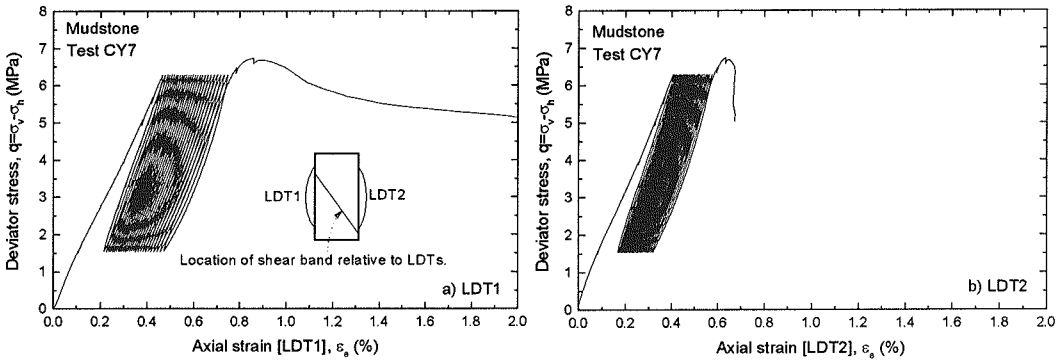

Fig.4. Stress-strain relationships for test CY7 on mudstone sample

Residual axial strains of silt-sandstone samples during undrained cyclic loading

On the silt-sandstone samples, six undrained cyclic triaxial tests were performed with different cyclic deviator stresses q_d, while maintaining the initial deviator stress q_0 constant at 1.96 MPa. Values of residual axial strains ε_r are plotted versus the number of cycles in Fig. 5. All the tests yielded gradual accumulation of ε_r throughout the undrained cyclic loading, and the rate of accumulation increased with the q_d value. Refer to Fig. 1 for results from test CS6 that showed the highest rate of accumulation.

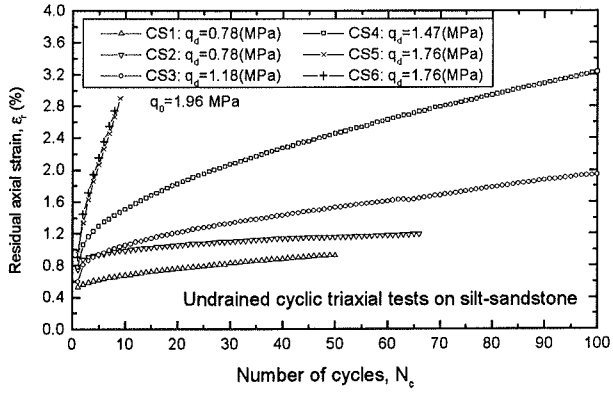

Fig.5. Accumulation of residual axial strains during cyclic loading on silt-sandstone samples

Figure 6 shows the stress-strain relationships for test CS1 that showed the lowest rate of accumulation of ε_r. As is similar to the case with Fig. 4, the axial strains measured with two LDTs were not largely different from each other, but the one measured with LDT2 that crossed the observed shear band (Fig. 6a) was generally larger than the other. The other test results showed similar trends within the measurable range of axial strains with LDTs (equal to about 2 %), suggesting no formation of shear band during the cyclic loading. It should be noted that, even in test CS1 at the lowest rate of accumulation of ε_r, the ε_r value approached to about 0.9 % during the undrained cyclic loading (Fig. 5). This value is much larger than the ε_r values at which the sudden large accumulation of the axial strain started in tests CY3 and CY5 on the mudstone samples (at ε_r of about 0.4 %, Fig. 2).

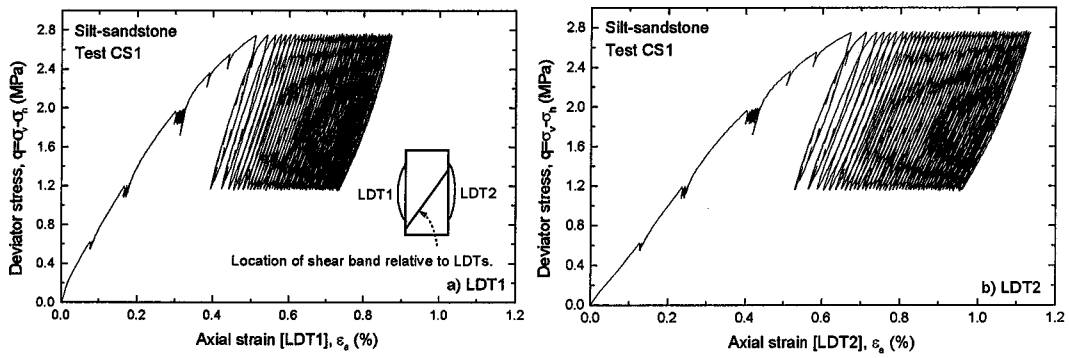

Fig.6. Stress-strain relationships for test CS1 on silt-sandstone sample

Figure 7 shows the effective stress path for test CS6 that showed the highest rate of accumulation of ε_r. Refer to Fig. 1 for the corresponding stress-strain relationship. During undrained cyclic loading, the excess pore water pressure did not accumulate on either the positive or the negative side. Similar trends of behavior were also observed in other tests including those on the mudstone samples.

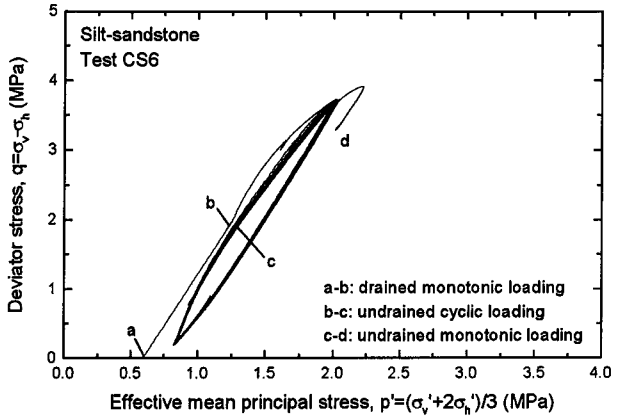

Fig.7. Effective stress path of test CS6 on silt-sandstone sample

Maximum deviator stress during undrained monotonic loading

Figures 8 and 9 show the relationships between the maximum deviator stress q_{max} during the undrained monotonic loading that was conducted after the undrained cyclic loading and the initial void ratio e_0 for the mudstone and silt-sandstone samples, respectively. In these figures, the value of q_0+q_d for each test was also indicated. It should be noted that, in tests CY3 and CY5 on mudstone samples where the axial strain accumulated largely during the undrained cyclic loading, the q_{max} values were set equal to q_0+q_d, since residual states were achieved during the last half cycle of undrained cyclic loading, as typically shown in Fig. 3. This behavior may be related with the possible formation of shear band during the cyclic loading as mentioned before.

For reference, test results without undrained cyclic loading history were added in Figs. 8 and 9. On the mudstone samples, the q_{max} value was not significantly affected by the undrained cyclic loading history, but it decreased in general with the increase in e_0. On the other hand, on the silt-sandstone samples, the q_{max} value was not clearly affected by the difference in e_0, while application of the undrained cyclic loading history resulted into increase in the q_{max} value. This behavior of the silt-sandstone samples seems quite peculiar, on which future investigations are required.

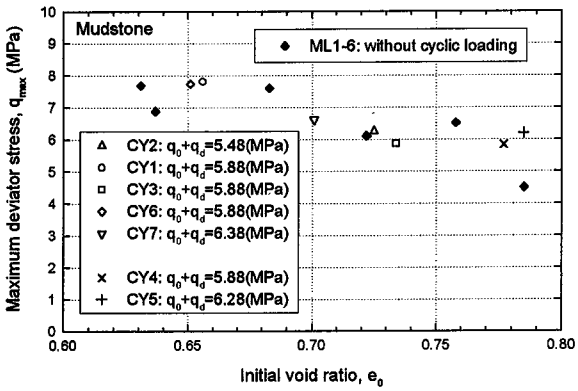

Fig.8. Maximum deviator stress during undrained monotonic loading on mudstone samples

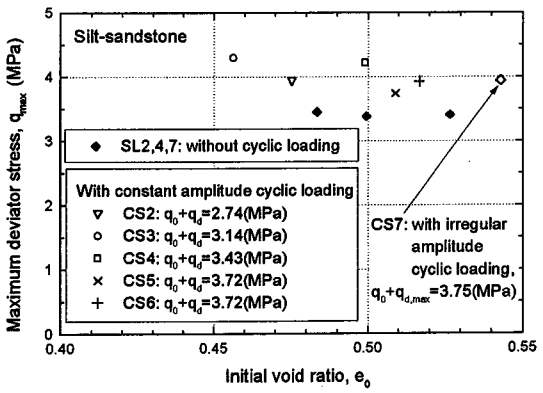

Fig.9. Maximum deviator stress during undrained monotonic loading on silt-sandstone samples

Discussion on strain increments during cyclic loading on silt-sandstone samples

On the silt-sandstone sample, an additional cyclic triaxial test (CS7) was conducted with increasing gradually the amplitude of cylic deviator stress (Fig. 10). When the stress-strain relationships are compared between Figs. 1 and 10, the following trends of behavior can be observed:

1) With the contant amplitude of cyclic deviator stress (Fig. 1), the increment of the residual axial strain was larger in the first cycle than in the subsequent cycles.
2) With the gradual increase in the amplitude of cyclic deviator stress (Fig. 10), the increment of the residual axial strain became larger in the later cycles. In particular, significant amount of axial strain was accumulated when the current deviator stress exceeded the ever-largest deviator stress level (i.e., the maximum deviator stress in the previous cycles). For example, during reloading from state e for the 7th cycle in Fig. 10, the increment of axial strain became much larger after exceeding the state f, which corresponds to the ever-largest deviator stress level during the preceding six cycles.

The above behaviors suggest that the increment of the residual axial strain consists of two components; the first one is the plastic strain increment $\Delta\varepsilon_i^p$ due to virgin loading that is mobilized after exceeding the ever-largest deviator stress; and the second one is the plastic strain increment $\Delta\varepsilon_{cy}^p$ due to cyclic loading that can be mobilized even before reaching the ever-largest deviator stress. In addition, the elastic strain increment $\Delta\varepsilon^e$ should also be considered in evaluating axial strains under different stress states. In the present study, these strain components were evaluated separately as briefly described in the next section.

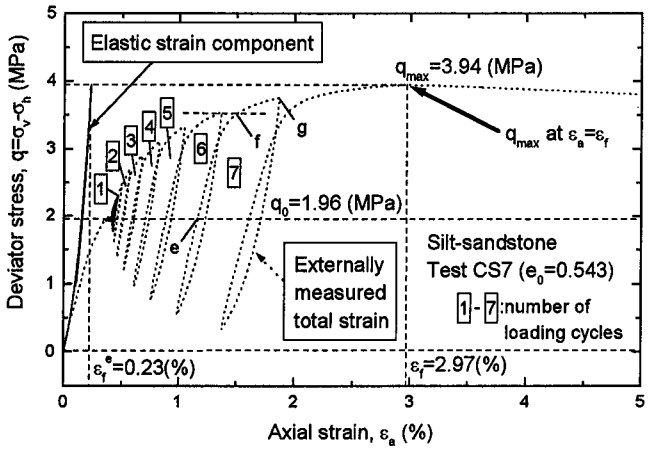

Fig.10. Stress-strain relationships for irregular cyclic loading test CS7 on silt-sandstone sample

Simulation of residual deformation behavior of silt-sandstone samples subjected to irregular cyclic loading

An attempt was made to simulate the accumulation of residual axial strain observed during the irregular cyclic loading test CS7 on the silt-sandstone sample.

The elastic strain increment $\Delta\varepsilon^e$ was evaluated based on the results from small amplitude axial loading and unloading conducted at several states during the isotropic re-consolidation, where the quasi-elastic vertical Young's moduli were modeled as a function of the current vertical effective stress. The elastic strain component evaluated by integrating the elastic strain increment is shown in Fig. 10.

The plastic strain increment $\Delta\varepsilon_{cy}^p$ due to cyclic loading was evaluated by applying the strain softening concept and the cumulative damage concept (Tatsuoka and Silver, 1981; Tatsuoka et al., 1986). The fatigue property of the tested silt-sandstone sample was formulated based on the results from the contant amplitude cyclic loading tests as:

$$\log(\Delta\varepsilon_{cy}^p) = a + b*\log(SR_d)$$
$$a = -0.712 + 1.15*\log(N_c)$$
$$b = 2.01 + 1.75*\log(N_c)$$

where, $\Delta\varepsilon_{cy}^p$ is the plastic strain value at the state of $q=q_0+q_d$ during each cycle; SR_d is a cyclic stress ratio defined as $q_d/(q_{max}-q_0)$; and N_c is the number of loading cycles.

Figure 11 compares the measured and modeled relationships between the cyclic stress ratio and the number of cycles inducing the strain increments of 0.1, 0.5, 1.0 and 1.5 %, respectively. Within the above strain range, the modeled relationships could reflect reasonably the trend of behavior observed in the measured ones. In analyzing the measured data, the plastic axial strain ε^p was evaluated by subtracting the elastic component from the measured total strain, from which the plastic strain increment during the first half cycle was deducted in order to exclude the effects of the virgin loading that was applied during the first quarter cycle; i.e., the origins of the plastic strain due to cyclic loading and the number of cycles were defined to be zero at state b' in Fig. 1.

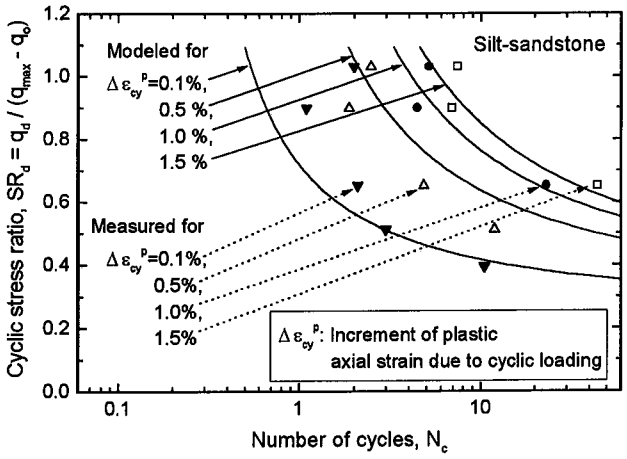

Fig.11. Relationships between cyclic stress ratio and number of cycles for silt-sandstone samples

The plastic strain increment $\Delta\varepsilon_i^p$ due to virgin loading was evaluated based on the results from monotonic loading tests without cyclic loading history. Figure 12 shows the relationships

between the normalized deviator stress q/q_{max} and the normalized plastic axial strain $\varepsilon^p/\varepsilon_f^p$, where ε_f^p is the plastic axial strain at $q=q_{max}$. Since the normalized relationship for test SL7 was different from those for tests SL2 and SL4, two cases of prediction of $\Delta\varepsilon_i^p$ were made based the normalized relationships obtained for tests SL4 and SL7, respectively. For example, the amount of $\Delta\varepsilon_i^p$ for the 7th cycle in test CS7 was evaluated from the $\varepsilon^p/\varepsilon_f^p$ values in Fig. 12 that correspond to the values of q/q_{max} at states f and g in Fig. 10, and the value of ε_f^p ($=\varepsilon_f-\varepsilon_f^e$ shown in Fig. 10).

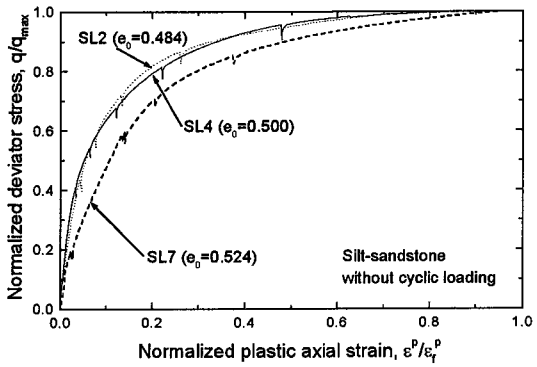

Fig.12. Normalized stress-strain relationships for monotonic loading tests on silt-sandstone samples

The amount of total axial strain ($=\Delta\varepsilon^e+\Delta\varepsilon_{cy}^p+\Delta\varepsilon_i^p$) defined at peak deviator stress state during each cycle (for example, at state g for the 7th cycle shown in Fig. 10) is compared between the measured and computed values in Fig. 13. The values computed based on the results from the monotonic loading test SL4 were well in accordance with the measured ones, while those based on the results from test SL 7 were generally larger than the measured ones. This is due to the softer response observed in the test SL7 than in the test SL4 as shown in Fig. 12. However, the general behavior on the rate of accumulation of the computed axial strain increments during each cycle were similar between these values and were consistent with the measured ones.

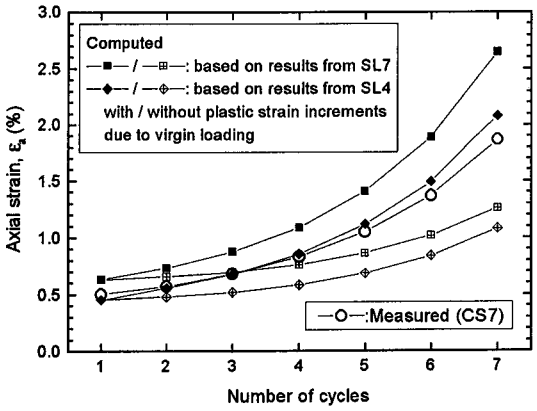

Fig.13. Comparison of computed and measured axial strains for test CS7 on silt-sandstone sample

For reference, the values computed without considering the accumulation of plastic strain increments $\Delta\varepsilon_i^P$ due to virgin loading except for the one during the first quarter cycle are also shown in Fig. 13. These values were generally smaller than the measured ones at later cyclic loading stages, suggesting the importance of considering such an accumulation of plastic strain increments $\Delta\varepsilon_i^P$ due to virgin loading. With the case of test CS7, the amount of $\Delta\varepsilon_i^P$ accumulated between the first and seventh cycles were about twice as large as the amount of $\Delta\varepsilon_{cy}^P$.

CONCLUSIONS

The results from cyclic triaxial tests on on two kinds of sedimentary softrocks could be summarized as follows.

1) The mudstone samples generally exhibited a limited amount of accumulation of residual axial strains during undrained cyclic loading. In such cases, it was estimated that the specimen suffered residual deformation relatively uniformly, while a limited extent of strain localization may have taken place within a region corresponding to the shear band that was formed in the subsequent monotonic loading stage. On the other hand, there were also cases where a sudden large accumulation of the axial strain was measured only with one LDT set in the region crossing the shear band, suggesting that the residual deformation may have taken place mainly within the shear band, which was possibly formed during the cyclic loading.
2) The silt-sandstone samples exhibited a gradual accumulation of residual axial strains during undrained cyclic loading. Even in the test that yielded the lowest rate of accumulation, the value of the residual axial strain became much larger than the one at which sudden large accumulation of the axial strain started in the tests on the mudstone samples, while the axial strain values measured with two LDTs remained to be similar to each other, suggesting no formation of shear band during the cyclic loading.
3) On the mudstone samples, the value of the maximum deviator stress q_{max} during undrained monotonic loading that was conducted after the undrained cyclic loading was not significantly affected by the cyclic loading history, but it decreased in general with the increase in the void ratio. On the other hand, on the silt-sandstone samples, the q_{max} value was not clearly affected by the difference in the void ratio, while application of the cyclic loading history resulted into increase in the q_{max} value.
4) The results from the tests on the silt-sandstone sample that was conducted with increasing gradually the amplitude of cylic deviator stress suggested that the increment of the residual axial strain consists of several components; the plastic strain increment $\Delta\varepsilon_i^P$ due to virgin loading that is mobilized after exceeding the ever-largest deviator stress; the plastic strain increment $\Delta\varepsilon_{cy}^P$ due to cyclic loading that can be mobilized even before reaching the ever-largest deviator stress; and the elastic strain increment $\Delta\varepsilon^e$. The

residual axial strains measured in this irregular loading test could be simulated reasonably by evaluating the $\Delta\varepsilon_{cy}^{p}$ component with applying the strain softening concept and the cumulative damage concept on the fatigue property that was formulated based on the results from contant amplitude cyclic loading tests, and by evaluating the $\Delta\varepsilon_{i}^{p}$ component based on the results from monotonic loading tests without cyclic loading history. The simulated amount of $\Delta\varepsilon_{i}^{p}$ accumulated between the first and seventh irregular loading cycles were about twice as large as the amount of $\Delta\varepsilon_{cy}^{p}$.

REFERENCES

Ampadu, S.K. and Tatsuoka, F. (1993): "Effects of setting method on the behavior of clays in triaxial compression from saturation to undrained shear," *Soils and Foundations*, No.33, Vol.2, pp.14-34.

Hayano, K., Matsumoto, M., Tatsuoka, F. and Koseki, J. (2001): "Evaluation of time-dependent deformation properties of sedimentary soft rock and their constitutive modeling," *Soils and Foundations*, No.41, Vol.2, pp.21-38.

Kashima, N., Fukunaga, S., Saeki, M. and Koseki, J. (2000): "Study on procedures to estimate earthquake-induced residual settlement of large scale bridge foundations (part 2)," *Proc. of 55th Annual Conf. of Japan Society of Civil Engineers*, Section 1.

Koseki, J., Moritani, T., Fukunaga, S., Tatsuoka, F. and Saeki, M. (2001): "Analysis on seismic performance of foundation for Akashi Kaikyo Bridge," *Pre-failure Deformation Characteristics of Geomaterials*, Jamiolkowski, Lancellotta and Lo Presti (eds.), Vol.2, pp.1405-1412.

Nakanishi, A., Ohkawa, T., Kaji, O. and Hosoda, Y. (1998): "Technology to develop a space in underground at a great depth," *Journal of the Japanese Geotechnical Society*, Vol.46, No.6, pp.17-20 (in Japanese).

Okamura, M., Matsuo, O. and Itabashi, T. (1999): "Cyclic triaxial tests on sedimentary soft rock from the Tokyo Bay," *Proc. of Symp. on Rotary Core Sampling of Soft Rocks and Hard Soils and Evaluation of Their Properties*, Japanese Geotechnical Society, pp.123-126 (in Japanese).

Tatsuoka, F. and Silver, M.L. (1981): "Undrained stress-strain behavior of sand under irregular loading," Soils and Foundations, Vol.21, No.1, pp.51-66.

Tatsuoka, F., Maeda, S., Ochi, K. and Fujii, S. (1986): "Prediction of cyclic undrained strength of sand subjected to irregular loadings," Soils and Foundations, Vol.26, No.2, pp.73-90.

Tatsuoka, F., Ochi, K., Tsubouchi, T., Kohata, Y. and Wang, L. (1997): "Sagamihara experimental underground excavations in sedimentary softrock," *Geotech. Engrg., Proc. of Institution of Civil Engineers*, 125, pp.206-223.

Yamagata, M., Yasuda, M., Nitta, A. and Yamamoto, S. (1996): "Effects on the Akashi Kaikyo Bridge," *Special Issue of Soils and Foundations on Geotechnical Aspects of the January 17 1995 Hyogoken-Nambu Earthquake*, pp.179-187.